NeuroImage 193 (2019) 146–156

Contents lists available at ScienceDirect

NeuroImage

journal homepage: www.elsevier.com/locate/neuroimage

A division of labor between power and phase coherence in encoding attention to stimulus streams

Alessandro Tavano [a,*], David Poeppel [a,b]

[a] Department of Neuroscience, Max Plank Institute for Empirical Aesthetics, Grüneburgweg 14, 60322, Frankfurt am Main, Germany
[b] Department of Psychology, New York University, 6 Washington Pl., 10003, New York City, New York, USA

ARTICLE INFO

Keywords:
Attention
Deviancy
Oscillation
Phase coherence
Reaction time

ABSTRACT

Both time-based (when) and feature-based (what) aspects of attention facilitate behavior, so it is natural to hypothesize additive effects. We tested this conjecture by recording response behavior and electroencephalographic (EEG) data to auditory pitch changes, embedded at different time lags in a continuous sound stream. Participants reacted more rapidly to larger rather than smaller feature change magnitudes (deviancy), as well as to changes appearing after longer rather than shorter waiting times (hazard rate of response times). However, the feature and time dimensions of attention separately contributed to response speed, with no significant interaction. Notably, phase coherence at low frequencies (delta and theta bands, 1–7 Hz) predominantly reflected attention capture by feature changes, while oscillatory power at higher frequency bands, alpha (8–12 Hz) and beta (13–25 Hz) reflected the orienting of attention in time. Power and phase coherence predicted different portions of response speed variance, suggesting a division of labor in encoding sensory attention in complex auditory scenes.

1. Introduction

Attention is typically distributed to different events, at different moments in time. Walking on a road, say, attention is captured by the dynamics of known events - e.g., the Doppler effect of passing cars – as well as by the onset of new events, such as a car honking. Both time-based and feature-based aspects of attention facilitate response behavior: for time-based effects, Bertelson and Boons (1960); Correa et al. (2004); Cui et al. (2009); Luce, 1986; Meck (1988); Niemi and Näätänen (1981); Nobre et al. (2007); Vangkilde et al. (2012); Woodrow (1914); for feature-based effects, Amenedo and Escera (2000); Berti and Schröger (2001); Tiitinen et al. (1994). It is thus natural to hypothesize an interaction: for example, the sudden onset of a car honk could capture more attention if the arrival of a car were expected, capitalizing on attention orienting in time. Alternatively, the mounting expectation that comes with temporal orienting might reduce feature-based attention capture for expected changes (Sussman et al., 2002).

Sensory surprise is formally studied as a function of the physical difference between repeated (standard) stimuli, and new (deviant) stimuli and classically measured using the oddball paradigm as the Mismatch Negativity response of the event-related potentials (ERPs, Näätänen, 1992; Näätänen et al., 2007). A common finding is that larger changes in feature facilitate stimulus detection by capturing more attention (Alho, 1992; Amenedo and Escera, 2000; Berti and Schröger, 2001; Tiitinen et al., 1994; Sussman, 2007). Salient changes in feature capture attention regardless of whether they disrupt a regularity or generate a new regularity (Southwell et al., 2016). It is unclear whether the same or different aspects of neural attention are involved in enhancing the encoding of sound change, a feature-based process, and the formation of a robust, standard memory trace, a time-based process(for a review, see Sussman et al., 2014). One difficulty in partitioning attention processes is inherent to the use of the oddball paradigm, in which neural responses to deviant events are overestimated relative to responses to standard events, the latter being suppressed by refractoriness (Ruhnau et al., 2012). Furthermore, the oddball paradigm confounds local standard statistics (e.g., number of repetitions before a deviant tone) with global standard statistics (i.e. the overall probability of standard stimuli).

To get around these limitations, we used a roving standard auditory paradigm (Baldeweg et al., 1999; Haenschel et al., 2005; Costa-faidella et al., 2011), in which each stimulus is repeated a variable number of times (standard formation process) before a change occurs (deviant stimulus), initiating a new repetition series. The roving standard paradigm thus highlights local standard statistics. Furthermore, as each new

* Corresponding author.
E-mail addresses: alessandro.tavano@ae.mpg.de (A. Tavano), david.poeppel@ae.mpg.de, david.poeppel@nyu.edu (D. Poeppel).

https://doi.org/10.1016/j.neuroimage.2019.03.018
Received 30 November 2018; Received in revised form 20 February 2019; Accepted 8 March 2019
Available online 12 March 2019

deviant eventually becomes a standard via repetition, the physical features of standards and deviants are matched by design. We parametrically varied standard sequence length in three steps – three-, six-, or nine-sound series – to study the neural encoding of orienting of attention in time to the next deviant relative to the magnitude – small or large – of deviancy.

With regard to feature-based attention processes, Barne et al. (2017) found that inter-trial phase coherence in the theta band (4–8 Hz) reflects the occurrence of unpredicted delays in action outcome, which resulted in a feedback-related negativity ERP signature. Makeig et al. (2002) suggested that event-related potentials mainly result from phase resetting of theta, alpha (8–12 Hz) and lower beta (14–20) ongoing oscillations (for lower beta phase reset as a rapid signal of deviant onset in a pre-attentive experimental setting, see Haenschel et al., 2000). Fuentemilla et al. (2006 and 2008), using three-tone trains, the last of which could be a deviant 50% of the times, found that both deviant and standard events are predominantly reflected by single-trial phase coherence, which was larger in the theta band (4–7 Hz), but extended into alpha territory. They did not report specific effects at lower frequencies. The contribution of oscillatory power to deviancy was significant but marginal, as phase coherence predicted both frontal and temporal generators of the Mismatch Negativity response. These mentioned studies were run pre-attentively, so the effect of attention is not known. However, given that attention has already been shown to increase inter-trial phase coherence of stimulus-driven neural response (Kim et al., 2007), we hypothesized that attention capture by feature changes in continuous streams would also modulate phase coherence. Furthermore, Lakatos et al. (2008) first showed that attentional selection may rely on the rhythmic changes in the excitability of neuronal ensembles, reflected by delta band phase.

With regard to time-based attention processes, the picture is more complex. Orienting attention in time to a target is reflected by modulations of oscillatory power within alpha (8–12 Hz) and beta (15–30 Hz) bands (de Lange et al., 2013; Morillon and Baillet, 2017). A seminal study (Rohenkohl and Nobre, 2011) used a foreperiod paradigm to show that oscillatory alpha power desynchronizes right before the onset of temporally predicted events, especially with long waiting times. The authors interpreted this finding as suggesting that alpha desynchronization regulates cortical excitation, by favoring motor response preparation. Notably, power desynchronization in the beta band occurs immediately after event onset in regular tone sequences (Fujioka et al., 2015), likely reflecting the release of motor programs from inhibition, in order to potentially initiate a motor response (e.g., button press; Joundi et al., 2013; Pfurtscheller et al., 2003: Pogosyan et al., 2009; Swann et al., 2009). We hypothesized that, as temporal expectancy grows with elapsed time to the next deviant event, oscillatory power in both the alpha and beta bands would decrease, relaying attentive and motor preparation processes. However, recent work indicates that phase concentration at very low frequencies (0.6–1.7 Hz) could also convey temporal expectations (Wilsch et al., 2015). In particular, in an auditory detection task, Stefanics et al. (2010) showed that reliably cued – predictable – onset of a target tone drives larger phase concentration in the delta band, suggesting a role for low frequencies in encoding expectancies.

2. Materials and methods

2.1. Participants

Participants were 30 right-handed young adults (age range 19–30, 8 males), self-reporting normal hearing, normal-to-corrected vision, no medical history of treatments affecting the central nervous system, no psychiatric disturbances and were compensated with 10 Euros per hour (duration 2 hs, including instruction, EEG montage, and cleaning). Sample size was calculated assuming *alpha* = 0.05, *power* = 0.80, mean difference for deviant N1 between small and large deviancy being 1.5 μV, SD = 2.8, using a paired *t*-test model. The experimental procedures were approved by the Ethics Committee of the Max Planck Society and undertaken with the written informed consent of each participant.

2.2. Experimental design

Participants sat comfortably in an IAC 40a sound attenuating and electrically shielded recording booth (IAC Acoustics), approximately 1 m from an LCD computer screen. There were two experimental sessions, separated by a brief rest period. In a *Pre-attentive* session, participants were instructed to direct the focus of attention to a silently presented movie projected on the computer screen while experimental sequences of pure tones were delivered diotically using electrodynamic headphones (Beyerdynamic DT 770 PRO). In an *Attentive* session, the same tone sequences were delivered, and participants were required to detect changes in either pitch or intensity as fast and as accurately as possible, while fixating a cross at the center of the computer screen. Participants used their right hand to respond to tone changes, pressing a pre-defined button on a Cedrus response box (Cedrus.com, response time jitter < 1 ms, measured with an oscilloscope). Prior to the Attentive experimental session, graphical depictions of the conditions were provided to aid with task completion. The order of Pre-attentive and Attentive sessions was counterbalanced across participants, and electroencephalographic (EEG) data were recorded for both sessions.

The experimental design followed the classic roving standard distribution of pure tones, with identical tones being repeated with a constant stimulus onset asynchrony (SOA) of 500 ms, until an unpredictable change in pitch or intensity sets up a new repetition series (*roving standard paradigm*, see Baldeweg et al., 1999; Haenschel et al., 2005). The first element of a new series is termed *deviant*, while the repetition series generates a standard trace: for convenience, we will call *standard* the last element of a repetition series. Experimental blocks containing changes in pitch were interleaved with blocks containing changes in intensity (see Fig. 1).

2.3. Stimulus structure

In the pitch change detection condition, stimuli were nine sine tones spaced from 440 to 1189 Hz in steps of 2 semitones in the equal tempered musical scale (duration = 50 ms, ramp/damp = 10 ms Tukey window, sampling frequency = 44.1 KHz). The sound pressure level (SPL) was individually calibrated for each transducer while using a temporal weighting suited for impulsive stimuli (tau = 35 ms), in order to equate loudness (= perceived intensity) across frequencies. To this end, we used an IEC 603184 artificial ear simulator (model G.R.A.S. 43AG) with pinnae and an IEC 60942 class 1 sound level calibrator (model Larson Davis CAL200).

In the intensity change detection condition, stimuli were nine sine tones spaced in steps of 3 dB SPL (four upward- and four downward-going, range: 3–21 dB SPL) around a central stimulus selected from the pitch change detection condition (= 698 Hz) and calibrated to 75 dB(A). However, since participants 1 to 9 reported difficulty in completing the task - obtaining very low hit rates -, for participants 11 to 30 the step size was increased to 6 dB SPL, and changes in intensity ranged between 6 and 42 dB SPL.

Changes in tone pitch or intensity occurred randomly after either *three, six,* or *nine* tones (standard sequence duration: 1.5 s, 3 s, and 4.5 s respectively), with the sole constraint that any deviant stimulus feature giving rise to a new standard sequence could not reappear before at least six other different stimulus sequences had appeared. There were 10 blocks per experimental condition, with each block containing 162 sine tones, amounting to 27 different standard sequences per block. At presentation, stimuli were further attenuated using a fixed −20 dB SPL step, resulting in a comfortable and perceptually controlled environment. Stimulus sequences were created using custom scripts written in Matlab (R2015b, 64 bits, mathworks.com). Stimulus delivery was controlled by

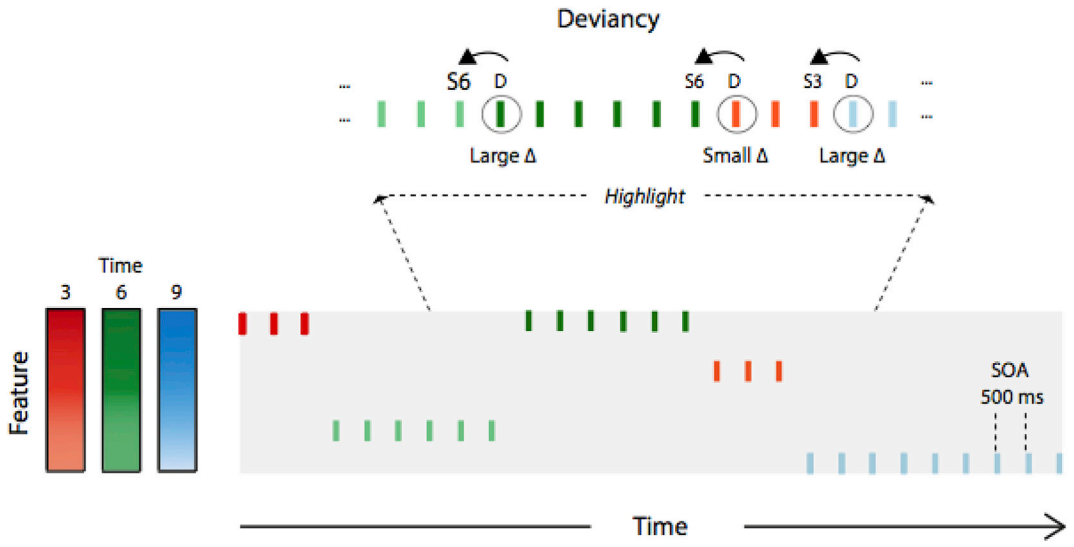

Fig. 1. Experimental design. Pure tones of 50-ms duration were isochronously delivered with a 500-ms stimulus onset asynchrony (SOA). Blocks contained tone sequences with changes in either pitch or intensity feature. Tone sequences were composed of three (red), six (green) or nine (blue) identical tones. Color gradients indicate standard sequences composed of low (dimmer hues) vs. high (darker hues) levels along a given feature dimension. Their combination gives rise to large or small Δ (deviant) events. The highlighted segment illustrates how each deviant tone at the beginning of a given sequence (D for Deviant) gives rise to a new repetition sequence, ending with a standard after 3 (S3), 6 (S6) or 9 tones (S9).

Psychophysics Toolbox Version 3 (PTB-3, psychtoolbox.org, Brainard, 1997; Pelli, 1997) for Matlab, running on a computer running Windows 7 (ASIO sound card for optimal stimulus latency control).

2.4. Peripheral physiology

Measurements of Autonomic Nervous System (ANS) functions were taken to test changes in autonomic arousal/motivation and stress between the Pre-attentive and Attentive sessions (Grings and Dawson, 1978). Participants' left hand laid still on a soft support, and a blood volume pulse (BVP) sensor (Brain Products) was placed on the ring finger. Changes in blood volume during cardiovascular activity modulate the amount of light that is absorbed by the blood vessel, which can be recorded as differences in the amount of reflection of an illuminating source. BVP is an indirect measure of heart rate, which should increase in response to arousing external stimuli. Participants also wore a respiratory belt (Brain Products) to measure the respiratory wave (RW). The frequency of the respiratory cycle should increase under stress, to allow for larger oxygen intake. BVP and RW times series were bandpass filtered between 12 and 240 beats per minute, and between 6 and 30 respiratory cycles per minute, respectively, and then subject to a peak detection procedure. BVP and RW rates were obtained for both experimental sessions using the reciprocal of the time difference between peaks, standardized and subject to a paired *t*-test to verify the effect of Attention. Results with $p \leq 0.05$ were declared significant. All analyses were run using custom Matlab scripts.

2.5. Behavioral data

In the Attentive session, pitch and intensity changes reflecting the physical difference of a deviant tone and last tone of the immediately preceding standard sequence, were recoded offline as either small or large deviancy events. In the pitch change condition, the small deviancy set included all events up to a 4-semitone difference, while the large deviancy set included all events at and above 8 semitones, regardless of the direction of pitch change (from low to high, from high to low). Events with a 6-semitone difference were randomly distributed between the small and large deviancy sets. In the intensity change condition, the small deviancy set included all events up to a 12 dB SPL difference, while the large deviancy set included all events at and above a 24 dB SPL difference. Events with 18-dB difference were randomly distributed between the small and large deviancy sets. Behavioral responses were considered valid if their latency with respect to deviant tone onset were equal to or larger than 200 ms (lower bound, insuring that participants react to deviant onset rather than anticipate it), and smaller than 1500 ms (higher bound, insuring comparability across standard durations). Accuracy was measured as the number of valid responses per condition that survived EEG epoching procedures (see below). A 2×3 repeated measures Analysis of Variance (rmANOVA, interaction model) was run on mean accuracy and response time measures obtained in the Attentive session with factors *Feature* (small deviancy vs. large deviancy) and *Time* (series of 3TONES vs. 6TONES vs. 9TONES). Significance was set at $p \leq 0.05$. Greenhouse-Geisser correction was applied whenever Mauchly's test signaled violation of the sphericity assumption. To assess the evidence for the alternative hypothesis relative to the null hypothesis, given the data, we estimated the Bayes factor (B_{10}) using Bayesian Information Criteria (Wagenmakers, 2007; JASP 0.8.0.1, jasp-stats.org).

2.6. EEG data preprocessing

Electroencephalographic (EEG) data were recorded using an actiCAP 32-channel, active electrode set (10–20 system, Brain Vision Recorder, Brain Products, brainproducts.com), at a sampling rate of 1 KHz, with a 0.1 Hz online filter (12 dB/octave roll-off). EEG recordings were offline downsampled to 250 Hz. There were 29 scalp electrodes, one electrode (originally, Oz) was placed on the tip of the nose, while two other electrodes (TP9 and TP10) acted as proxy for mastoid electrodes (10–20 system). All impedances were kept below 5 kOhm, except for the nose electrode, which was kept below ~10 kΩ. Since electrode placement on the tip of the nose was suboptimal in a subset of participants, and sometimes detached from the skin during recording, the data of all participants were off-line re-referenced to the digitally linked mastoid proxies. EEG data was further preprocessed using the EEGLAB toolbox for Matlab (Delorme and Makeig, 2004; sccn.ucsd.edu). Continuous EEG data were visually inspected to remove large non-stereotypical artefacts (e.g., sudden head movements, chewing), digitally filtered 0.5 Hz high-pass and 45 Hz low-pass (Kaiser window, beta = 5.65326, filter orders 909 and 93, transition bandwidths 1 and 10 Hz for high- and

low-pass, respectively), and submitted to an Independent Component Analysis using Infomax (Bell and Sejnowski, 1995). Infomax maximizes the statistical independence of input components, allowing for optimal source separation. The Independent Components (ICs) were further tested for extremely large amplitude fluctuations (measured via kurtosis of activity) within 1-s-long dummy epochs, using a recursive algorithm starting at a threshold of 12 standard deviations and adaptively incrementing/reducing it at each iteration (max rejection per iteration: 5% of data; max 4 iterations). There resulted a cleaned set which was submitted to a second Infomax ICA pass, this time with the option extended, which enhances the chance of capturing sub- and super-Gaussian signals (Jung et al., 1998). Using the SASICA toolbox for EEGLAB (Chaumon et al., 2015), ICs reflecting blinks/vertical eye movements and lateral eye movements were detected by a correlation threshold of 0.7 with bipolarized F4-Fp2 and F8—F7, respectively, and found to be present in all participants (range: 1–3 ICs for vertical, 1–2 ICs for horizontal). To reduce inter-trial signal variability, ICs likely to reflect muscle artefacts were also identified, using autocorrelation (threshold = 0, lag = 20 s), while for ICs potentially reflecting bad electrodes a measure of focal topography was used (threshold at 7 standard deviations relative to the mean across electrodes). Additionally, ICs reflecting heartbeat, when detected, were selected for rejection. The ICA results were then copied back to the original EEG datasets and rejected before epoching. For all single-trial analyses, EEG recordings were then filtered 0.2 Hz high-pass and 40 Hz low-pass (Kaiser window, beta = 5.65326, filter order 2267 and 909 points, transition bandwidth 0.4 and 1 Hz, respectively).

2.7. Time-frequency analysis

Prior to analyzing the experimental data, we checked for the presence of significant differences in occipital alpha band (8–12 Hz) global power between Pre-attentive and Attentive sessions, as they differed in task-unrelated visual stimulation. We calculated the average global power spectrum using a Fast Fourier Transform (Hanning window) on detrended dummy epochs extracted every 1 s across the entire session data, filtered at 1 Hz high-pass. Power spectra were obtained by squaring the absolute values of the complex Fourier coefficients, after correcting for the Hanning window (2/sqrt (1.5)). Statistical analyses were performed on normalized amplitudes of the averaged occipital electrodes (O1, O2), obtained by dividing the power spectrum by length of the time domain signal.

To test which component of the neural signal predicted the feature component of behavior, we first focused on the Attentive session. We applied a single-trial analysis of the global power spectrum and inter-trial phase coherence for small vs. large feature change, occurring after 3TONES, 6TONES and 9TONES, extracted from the Attentive session. Epochs were cut around deviant onset (1-s long: 500 to 500 ms). We analyzed only epochs which contributed to signal-to-noise ratio (Rahne et al., 2008). Individual epochs were not baseline-corrected: first and foremost, baselining the deviant relative to the standard would confound local standard and deviant effects; second, baselining invalidates voltage topography analysis (Urbach and Kutas, 2006); third, applying appropriate high-pass filtering instead of baseline correction is nowadays technically preferable to remove very low frequency artefacts (Widmann et al., 2015). To control for eventual slight differences in noise due to epoch number among conditions, epoch number was equated before running statistical comparisons. Time-frequency analyses were run using the Fieldtrip toolbox for Matlab (Oostenveld et al., 2011; www.ru.nl/neuroimaging/fieldtrip), and custom Matlab scripts. We obtained oscillatory power and complex Fourier spectrum estimates – the latter used to calculate inter-trial phase coherence - at each sensor by multiplying each time sample with a Morlet wavelet in the frequency domain (0.25 Hz resolution, from 0.25 to 35 Hz; 'mtmconvol' calculation method in Fieldtrip, Hanning window), in steps of 200 ms. Phase coherence was computed using the Inter-Trial Phase Coherence index (ITPC), analogous to the "phase-resetting index" (Tallon-Baudry et al., 1996). The Fourier output was amplitude-normalized, angles were summated, and normalized by length. ITPC values range from 0 to 1, with values near 1 implying almost perfect phase coincidence across trials. Comparisons between small vs. large deviancy epochs at each standard series level (3TONES, 6TONES and 9TONES), at each individual electrode and time point, were run using a nonparametric, cluster-based permutation test, which controls for the family-wise error rate within each comparison (Maris and Oostenveld, 2007). This approach does not require a priori assumptions about the time and frequency windows likely to show a difference between conditions (minimal N electrodes per cluster = 2, cluster parameter = maxsize, 2000 permutations, significance set at 0.05, two-sided). We selected all time-frequency samples reflecting a significant difference between small and large deviancy across the scalp, and used it as a spatial filter to obtain maps of the distribution of voltage at each standard series level. These were contrasted by using a topographic analysis of variance, which calculates the degree of dissimilarity between two conditions as the squared difference of voltage values normalized by the global field power at each electrode and time point, and tests for significance using a resampling approach (TANOVA, Murray et al., 2008). The mean values collected at electrodes with the largest activity into a multiple regression model as predictors of behavior with factors *Time* (series of 3TONES vs. 6TONES vs. 9TONES), and *Feature* (small Δ vs. large Δ). Significance was set at $p \leq 0.05$. Bonferroni correction was applied to correct for family-wise error across multiple comparisons. Here too, we estimated the Bayes factor (B_{10}).

We then concentrated on attention *per se*, by including in the model the data from the Pre-attentive condition. To isolate the effect of attention on feature-based sensory processing, we included in the single-trial analysis small vs. large feature change, occurring after 3TONES, 6TONES and 9TONES, extracted from the Pre-attentive session. The experimental sequences were the same for the Attentive and the Pre-attentive sessions, thereby permitting to factor away the impact of stimulus distribution. Again, we ran a nonparametric, cluster-based permutation test, this time contrasting Attentive vs. Pre-attentive single-trial neural estimates for standard sequences with 3TONES, 6TONES and 9TONES, 3TONES, 6TONES and 9TONES for small and large deviancy events. The results were then entered into a 2 × 3 x 2 repeated measures Analysis of Variance (rmANOVA, interaction model) with factors *Attention* (Pre-attentive Δ vs. Attentive), *Time* (series of 3TONES vs. 6TONES vs. 9TONES), and *Feature* (small Δ vs. large Δ). Significance was set at $p \leq 0.05$. Greenhaus-Geisser correction was applied whenever Mauchly's test signaled violation of the sphericity assumption. The mean difference between Attentive and Pre-attentive neural activity at electrodes with the largest activity was again entered into a multiple regression model with factors *Time* (series of 3TONES vs. 6TONES vs. 9TONES), and *Feature* (small Δ vs. large Δ), and response behavior as a dependent measure. Significance was set at $p \leq 0.05$. Bonferroni correction was applied whenever required.

As for the orienting of attention in time, we analyzed single-trial epochs reflecting standard sequence duration, extracted from the Pre-attentive and Attentive sessions, cut around the inter-deviant interval (1.5 s for 3 sounds, 3 s for 6 sounds, and 4.5 s for 9 sounds, plus 500 ms at the beginning and end of each standard series). Notice that these long epochs reflect the mounting of temporal expectations regardless of whether the subsequent or preceding feature change was large or small. The effect of attention was measured at each standard series level (3TONES, 6TONES and 9TONES) once more using a nonparametric, cluster-based permutation test, for both power and phase coherence. To capture the evolution in time of frequency bands that significantly differed between the Attentive and Pre-attentive conditions, we standardized and averaged their neural profile, and run two-way rmANOVAs with factors *Attention* and *Time* to test for effects on the last tone of each sequence (Standard; Bonferroni-corrected, $p \leq 0.05$). Finally, we plugged phase coherence and power envelope estimates for both deviant and standard tones into a multiple regression analysis as single-trial predictors of response speed.

2.8. Data and code availability

The data and code, which support the findings of this study, comply with the requirements of the Max Planck Society, and with the institutional ethics approval. They are available from the corresponding author upon reasonable request, for research purposes only.

3. Results

3.1. Peripheral physiology responses

A preliminary data review showed that, even with a 6 dB intensity step, the intensity change condition did not result in a sufficient number of trials in all conditions. Thus, we report only data from the pitch change condition. Attention to stimuli significantly changed heartbeat rate ($t_{(1,29)} = -2.62$, $p = 0.01$). Standardized values show an increase of heartbeat frequency – indexing autonomic arousal – in the Attentive condition relative to the Pre-Attentive condition (Pre-Attentive, mean = -0.0014, Standard Error of the Mean, SEM = 0.0007; Attentive, mean = 0.0011, SEM = 0.0006). There was no significant difference in stress-related respiratory frequency: $t_{(1,29)} < -1.00$, $p = 0.32$.

3.2. Behavioral responses

Two participants (1, 14) had an extremely low number of correct detections (N < 10) in one or more conditions and were thus excluded from further analysis. Individual response time profiles were deemed as valid based on a 95% Confidence Interval (CI) range, leading to the exclusion of participants # 5, 20 and 30 as upper-bound outliers (Ratcliff, 1993). For the remaining 25 participants, the mean number of correct detections per condition ranged between 40.44 and 43.36 (SEM range = 0.81–1.10), within each session.

We ran a 2 × 3 rmANOVA with factors Feature (small vs. large deviancy) and Time (three temporal expectation levels: 3TONES, 6TONES, 9TONES) on correct detections and found a main effect of Time (F (2,48) = 6.52, $p < 0.01$, $\eta^2 = 0.24$). Accuracy improved with mounting temporal expectation, regardless of deviancy magnitude: theoretical maximum = 45, mean 3TONES = 40.37 (SEM = 0.95), mean 6TONES = 41.30 (SEM = 0.97), mean 9TONES = 42.04 (SEM = 1.08). A rmANOVA with Feature and Time factors on median response times (RT) showed a significant effect of Feature (F (1,24) = 51.77, $p < 0.001$, $\eta^2 = 0.68$), and a significant effect of Time (F (2,48) = 73.91, $p < 0.001$, $\eta^2 = 0.75$). Participants were faster at detecting deviant events arising from large deviancy events (mean = 312.24 ms, SEM = 9.39) rather than small ones (mean = 345 ms, SEM = 7.96). A hazard rate-like distribution of response times also emerged. Waiting for 6TONES or 9TONES led to faster responses than waiting for 3TONES (all ts (1,24) > 9.98, all $ps < 0.001$, Bonferroni corrected), although waiting for 9TONES or 6TONES did not have significantly different effects (t (1,24) = 1.01, $p = 0.57$): mean RT 3TONES = 370.54 ms (SEM = 11.48), mean RT 6TONES = 310.69 ms (SEM = 7.37), mean RT 9TONES = 304.64 ms (SEM = 7.90). The interaction of Feature and Time factors was not significant (F (2,48) = 0.26, $p = 0.76$; see Fig. 2A). To evaluate the amount of evidence for including the interaction term from the statistical model given the experimental results, we calculated the Bayes factor (B10). We

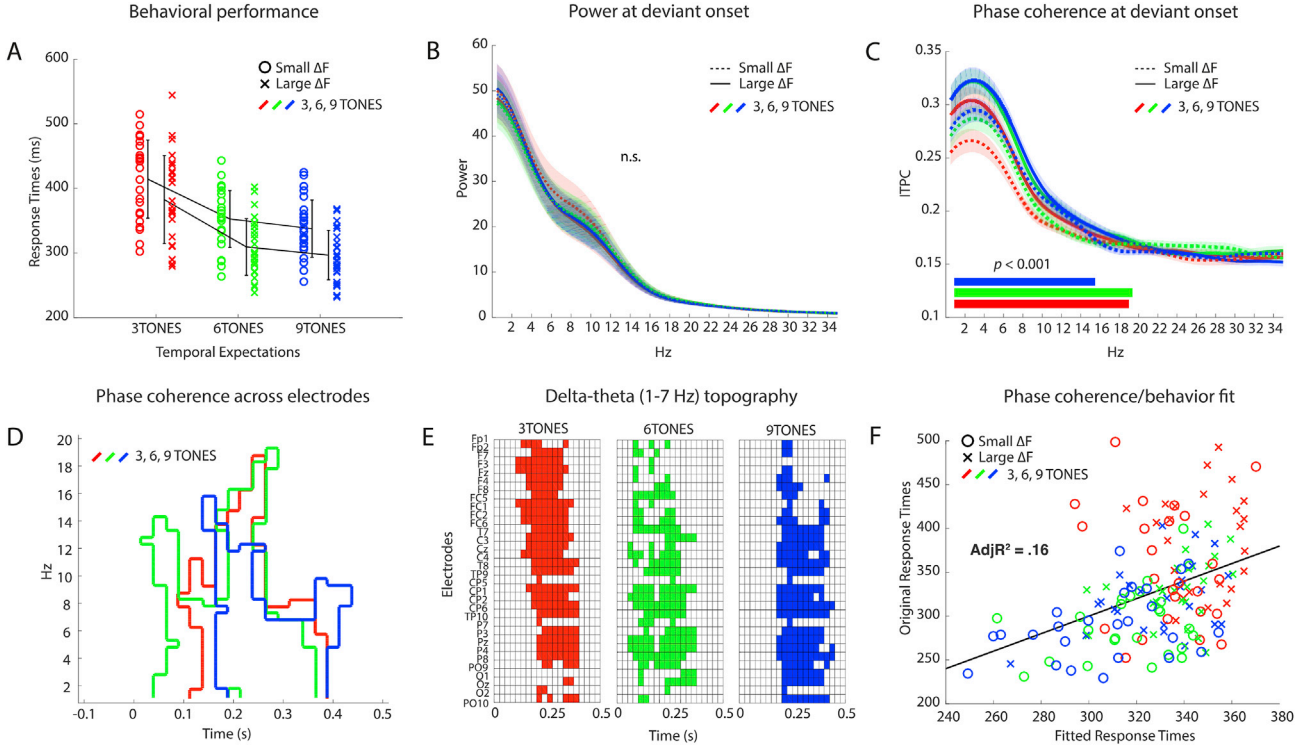

Fig. 2. A. Mean response times for the Attentive condition. Three, six and nine tone sequences are color-coded in red, green and blue, respectively. Small and large deviancy events are plotted separately. Error bars indicate standard deviation. B. Power profile in all conditions, from 1 to 35 Hz, averaged across all electrodes. No significant difference was found when comparing large vs. small deviancy events at any temporal expectation level. Shaded areas indicate standard error of the mean. C. Phase coherence profile resulting from the average across all electrodes. Shaded areas indicate standard error of the mean. Significant cluster-based differences up to the lower beta range (<20 Hz) – reported as color-coded horizontal bars – were found between large and small deviancy events at all temporal expectation levels. D. Significant cluster-based differences depicted in the time-frequency dimension, disregarding the magnitude of phase coherence. Notice that the clusters largely overlap between ~150 and ~400 ms, and up to 12 Hz, the upper bound of alpha frequency band. The largest overlap is localized to the delta (1–4 Hz) and theta (5–7 Hz) bands. E. Topographical distribution of significant clusters 1–7 Hz across time. F. Brain-behavior fit between phase coherence at deviant onset as a predictor and response speed. Fitted response times are plotted against original response times to highlight the strength of the predictive relationship.

found that the evidence against the null hypothesis was 10.14 times higher (Cauchy prior width = 0.707), and thus more compelling, without the interaction term (B10 Time + Feature = 7.132e+12; B10 Time + Feature + Time*Feature = 7.033e+11). We conclude that the factors Time and Feature independently modulated response speed.

3.3. Neural signatures of deviancy and temporal expectations

We first checked for the presence of confounding effects in task-irrelevant neural activity, potentially driven by differences in visual stimulation between the Attentive and Preattentive conditions. We calculated the average power spectrum at occipital sites, and there was no significant difference: t (1,24) = −0.53, $p = 0.59$; mean Pre-attentive = 0.10 μV^2 (SEM = 0.02), mean Attentive = 0.11 μV^2 (SEM = 0.02).

As for task-relevant brain activity in the Attentive condition, we compared oscillatory power in the window from 0 to 500 ms post-stimulus around deviant onset between small and large deviancy events, at each temporal expectation level, for frequencies 1–35 Hz. No significant time-frequency cluster of differences emerged, suggesting that deviancy was not encoded by changes in power spectrum (all $ps \geq 0.067$). The power profile in Fig. 2B illustrates this point, by displaying the average values across electrodes, with a typical deflection in the theta/alpha (5–12 Hz) band range. As a further test, we entered the time-frequency results in the theta and alpha bands (averaged across all electrodes, time and frequency bins) in a 2 × 3 rmANOVA with factors Feature and Time: there was no main effect and no significant interaction (all $Fs < 1.8$, all $ps > 0.19$), suggesting that power estimates at deviant onset were not sensitive to either experimental manipulation. Second, we analyzed inter-trial phase coherence. We found positive clusters of significant differences between large vs. small deviancy events, at all temporal expectation levels (all $Ts \geq 1805$, all $ps < 0.001$, Bonferroni corrected). No significant negative clusters were found (all $ps > 0.06$). Fig. 2C displays the spectral profile of phase coherence at each experimental condition, averaged across all electrodes, highlighting the extent of cluster-based significance for each comparison in the frequency dimension via color-coded horizontal bars. Fig. 2D presents the same data, this time disregarding the magnitude of the effects and focusing instead on the extension in time of significant clusters, and their morphology in the frequency domain. Significant clusters were larger for delta and theta bands (1–7 Hz; 3TONES, from 152 to 376 ms; 6TONEs, from 24 to 352 ms; 9TONES, from 176 to 376 ms), although they extended into the alpha and lower beta bands (up to 20 Hz), as well, particularly at latencies traditionally corresponding to the Mismatch Negativity (~200 ms; Näätänen et al., 2007; Tiitinen et al., 1994). Plotted clusters include all significant time-frequency bins, at all scalp channels. A topographical analysis of variance for the delta and theta frequencies showed that temporal expectations do not significantly change the underlying generators of feature-based differences (TANOVA, all $ps > 0.15$). Fig. 2E illustrates this point by collapsing all significant bins across frequencies in the interval between 0 and 500 ms. We calculated the average phase coherence values for the combined delta/theta bands (1–7 Hz) between deviant onset and 500 ms post-onset, for all channels. These estimates were entered in a 2 × 3 rmANOVA with factors Feature and Time. Similarly to behavioral data, we found a main effect of Feature (F (1,24) = 132.39, $p < 0.001$, $\eta^2 = 0.84$), and a main effect of Time (F (2,48) = 8.87, p < 0.001, $\eta^2 = 0.27$), but no significant interaction (F (2,48) = 0.14, $p = 0.87$). Phase coherence was larger for large deviancy magnitudes (mean = 0.38, SEM = 0.02) than for small deviancy magnitudes (mean = 0.27, SEM = 0.01). Waiting for 6TONES or 9TONES led to larger phase coherence than waiting for 3TONES (all ts (1,24) > 2.55, all $ps < 0.05$, all p-values Bonferroni corrected), but phase coherence to deviant onset after 9TONES was similar to phase coherence after 6TONES (t (1,24) = 1.69, $p = 0.10$): mean ITPC 3TONES = 0.30 (SEM = 0.01), mean RT 6TONES = 0.33 (SEM = 0.01), mean ITPC 9TONES = 0.36 (SEM = 0.02). The evidence against the null hypothesis was 14.9 times higher (Cauchy prior width = 0.707), and thus more compelling, without the interaction term (B10 Time + Feature = 1.796e+19; B10 Time + Feature + Time*Feature = 1.198e+18). The estimates of phase coherence at delta-theta bands (1–7 Hz) were used as a predictor of behavior. The resulting linear regression model was significant (F (1,148) = 28.26, p < 0.001, see Fig. 2F). This is consistent with our hypothesis that phase coherence at low frequencies is a better predictor of deviancy magnitude than power. However, we found it also reflects the topographic and magnitude changes induced by temporal expectations. The adjusted R^2 was equal to 0.16, suggesting the model explained a small-to-moderate part of the variance.

3.4. Attention on feature change

In the Attentive session, the distribution of response times depends on attention and stimulus structure. We highlighted the effects of attention *per se*, while abstracting from stimulus structure, by comparing the same deviant epochs from the Attentive (focus on stimuli) and the Pre-attentive (focus on silenced movie) sessions.

The comparison of power estimates for deviant onset in the Attentive and Pre-attentive conditions highlighted large positive clusters of significant differences for both small and large deviancy magnitudes, and at each temporal expectation level (all $Ts > 17652$, all $ps < 0.05$, Bonferroni corrected). No significant negative clusters were found (all $ps > 0.12$). The distribution of positive clusters overlapped in frequency (≤20 Hz) in the post-stimulus period; however, significance began before deviant onset, likely reflecting the focus of attention on continuous auditory stimulation, rather than deviancy proper. Fig. 3A depicts the spectral profile of each condition, averaged across all electrodes, for frequencies 1–35 Hz in the post-stimulus period. When estimates of power for significant electrode and time-frequency bins between 1 and 20 Hz were entered in a 2 × 2 x 3 rmANOVA, with factors Attention (Pre-attentive vs. Attentive), Feature (small vs. large deviancy) and Time (three temporal expectation levels: 3TONES, 6TONES, 9TONES), there resulted a significant effect of Attention (F (1,24) = 11.05, $p < 0.01$, $\eta^2 = 0.35$), but no significant effects of Time or Feature factor, and no significant interactions (all $Fs < 3.25$, all $ps > 0.08$). Average power was larger in the Attentive condition (mean = 18.79 μV^2, SEM = 1.64), than in the Pre-attentive one (mean = 13.28 μV^2, SEM = 2.77).

As for inter-trial phase coherence, we also found extended significant positive time-frequency clusters reflecting the effect of attention in all conditions (all $Ts > 2630$, all ps < 0.01, Bonferroni corrected). No significant negative clusters were found (all $ps > 0.10$). The effects of attention began early after deviant onset (mean cluster onset = 100 ms), and involved frequencies up to ~15 Hz. Fig. 3B and C illustrate the average values of inter-trial phase coherence across all electrodes, collected for small deviant event and large deviant events, respectively. The largest differences between Attentive and Pre-attentive trials were localized at delta and theta frequencies (1–7 Hz; color-coded, horizontal bars). Fig. 3D illustrates the topographical distribution of significant cluster differences (t-values) between Attentive and Pre-attentive trials for phase coherence at combined delta and theta bands, highlighting a parietal concentration of significant attention effects. Topographies reflect the cluster t-value averages within 150 ms and 250 ms post-onset. We then submitted the estimates of average phase coherence at delta and theta frequencies for all significant time-frequency bins, averaged across all significant electrodes, to a 2 × 2 x 3 rmANOVA with factors Attention (Pre-attentive vs. Attentive), Feature (small vs. large deviancy) and Time (three temporal expectation levels: 3TONES, 6TONES, 9TONES). Results show main effects for all three factors: Attention, F (1,24) = 63.33, $p < 0.001$, $\eta^2 = 0.72$; Feature, F (1,24) = 37.80, $p < 0.001$, $\eta^2 = 0.61$; and Time, F (2,48) = 5.72, $p < 0.01$, $\eta^2 = 0.19$. Attention separately interacted with the Feature factor (F (1,24) = 18.05, $p < 0.001$, $\eta^2 = 0.42$) and the Time factor (F (2,48) = 11.83, $p < 0.001$, $\eta^2 = 0.33$). Attention amplified the difference in phase coherence between large and small deviancy events: Pre-attentive, t (1,24) = 3.12, $p < 0.01$ (large Δ, mean = 0.26, SEM = 0.01; small Δ: mean = 0.19, SEM = 0.005);

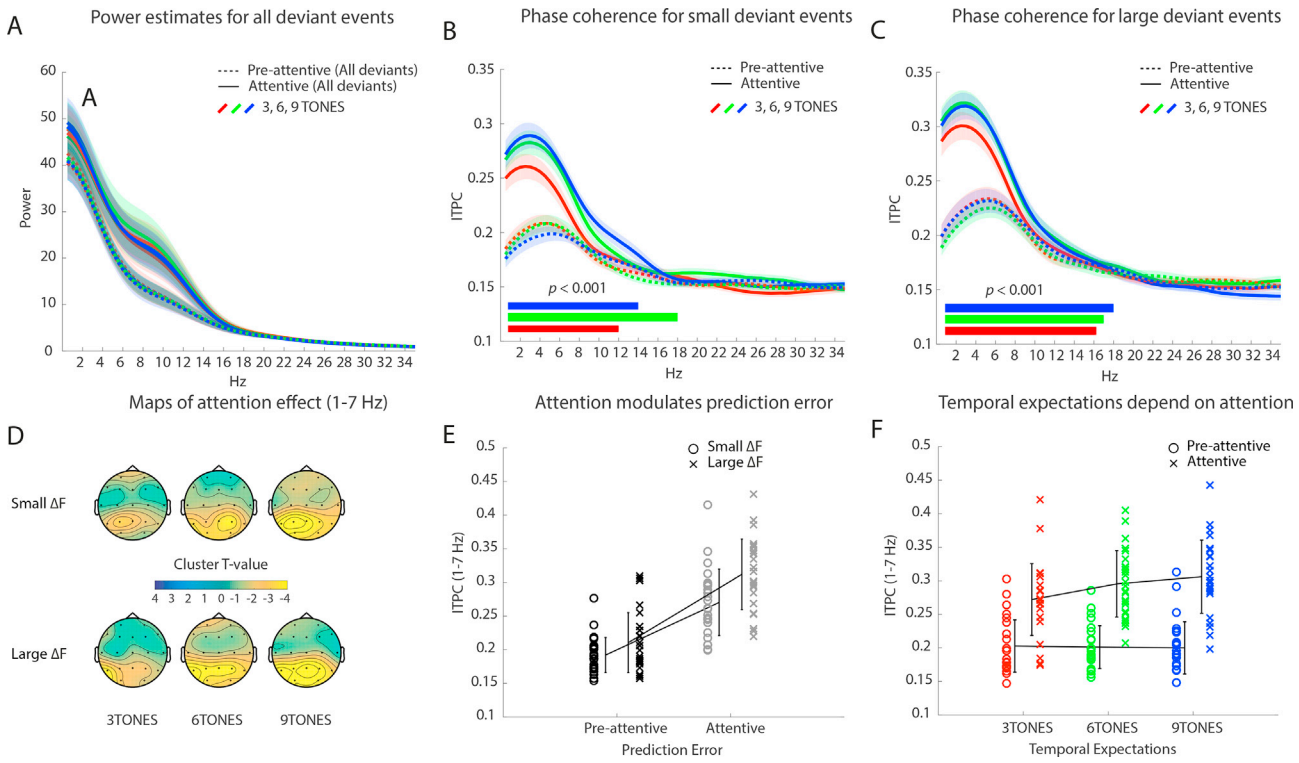

Fig. 3. Attention modulates power and phase coherence at deviant onset. A. Color-coded power profile for all conditions, averaged across all electrodes (pre- and post-onset). Shaded areas indicate standard error of the mean. The figure highlights the difference between Attentive and Pre-attentive conditions, eliminating the difference between small and large deviancy events. B & C. Phase coherence amplitudes, averaged across all electrodes, for small and large deviants in the Attentive and Pre-attentive conditions. Horizontal bars indicate the extension of significant clusters reflecting the effect of Attention in the frequency domain. D. Topographic plots of cluster values (mean of values between 150 and 250 ms post-onset, reflecting the typical latency range of the Mismatch Negativity, Näätänen et al., 2007; Tiitinen et al., 1994), highlighting the parietal concentration of significant differences. E. Interaction between Attention and Feature factors, showing that attention magnifies the difference in phase coherence between large and small deviant events. F. Interaction between Attention and Time factors, showing that temporal expectations modulated phase coherence only under focused attention.

Attentive, t (1,24) = 7.49, p < 0.001 (large Δ: mean = 0.30, SEM = 0.01; small Δ: mean = 0.21, SEM = 0.01; Bonferroni corrected, see Fig. 3E). Importantly, only in the Attentive condition did temporal expectations modulate phase coherence (Fig. 3F): Waiting for either 6TONES or 9TONES led to larger phase coherence values than waiting for 3TONES (all ts (1,24) = 3.46, $p < 0.01$, Bonferroni corrected), while all other comparisons were not significant, all $ps > 0.13$): mean ITPC 3TONES in the Attentive condition = 0.26 (SEM = 0.01), mean RT 6TONES = 0.29 (SEM = 0.01), mean ITPC 9TONES = 0.30 (SEM = 0.01). There was no effect of temporal expectations in the Pre-attentive condition (all $ps > 0.25$). However, there was no significant three-way interaction and, specifically, no significant interaction of Feature and Time factors (all $Fs < 0.45$, all $ps > 0.63$), suggesting that the neural underpinnings of Feature and Time aspects of attention to stimulus change within complex streams are distinct. We then entered phase coherence and power estimates as predictors of response times, using a multiple linear regression. A significant model emerged explaining a moderate portion of variance (F (1,148) = 21.16, $p < 0.001$, adjusted$R^2 = 0.21$), with only phase coherence as a significant predictor ($p < 0.001$; global power, $p = 0.06$).

3.5. Orienting attention in time

We then investigated the deployment of attention along the three steps of waiting time for deviant onset (3-, 6-, and 9-tone series), averaging across the Feature dimension. We analyzed epochs of 1.5, 3 and 4.5 s time locked to the next deviant onset, with additional 1-s segments at either side. We first looked at phase coherence, and found large positive clusters at the onset of all deviant tones (beginning and end of each epoch), thereby replicating our findings (all $Ts > 9770$, all $ps < 0.001$; see Fig. 4A; phase coherence is depicted by black contours plots). There were no significant negative clusters (all $ps > 0.08$). However, we found no significant cluster in the waiting time period, with the exception of the 9TONES series, for which there resulted a significant cluster at the onset of the last tone (Standard, $p < 0.01$). This suggests that phase concentration does not track the incremental nature of waiting time, but – if at all – it reflects certainty about the subsequent onset of a deviant sound. We then looked at global power and found continuous attention effects clustering strongly at alpha (8–12 Hz) and beta (13–25 Hz) bands. There was one large, significant positive cluster for each waiting series (all $Ts \geq 153166$, all $ps < 0.005$, Bonferroni corrected). There were no negative clusters (all $ps > 0.17$). Fig. 4A plots the significant cluster values for the three different temporal expectation levels, at the exemplar electrode Pz, time-locked to the onset of the following deviant. Notice that, regardless of tone series length, deviant onset (D) caused a change in which frequency bands reflected power-based attention, from alpha/beta into delta/theta, followed by a rebound at first tone repetition (S2), and sustained larger global power difference in the alpha/beta range for the remaining of each waiting time series. We calculated standardized estimates of average alpha (8–12 Hz) and beta (13–25 Hz) bands across all electrodes and time-frequency bins, and subtracted the activity in the Pre-attentive condition from that in the Attentive condition. Fig. 4B displays the average values across all electrodes, and shows that deviant onset is characterized by a rapid suppression of both the alpha and beta rhythms, after an initial alpha power burst. Notice that at all temporal expectation levels, mean alpha band power was significantly larger than mean beta band power between 200 ms and 600 ms after deviant onset.

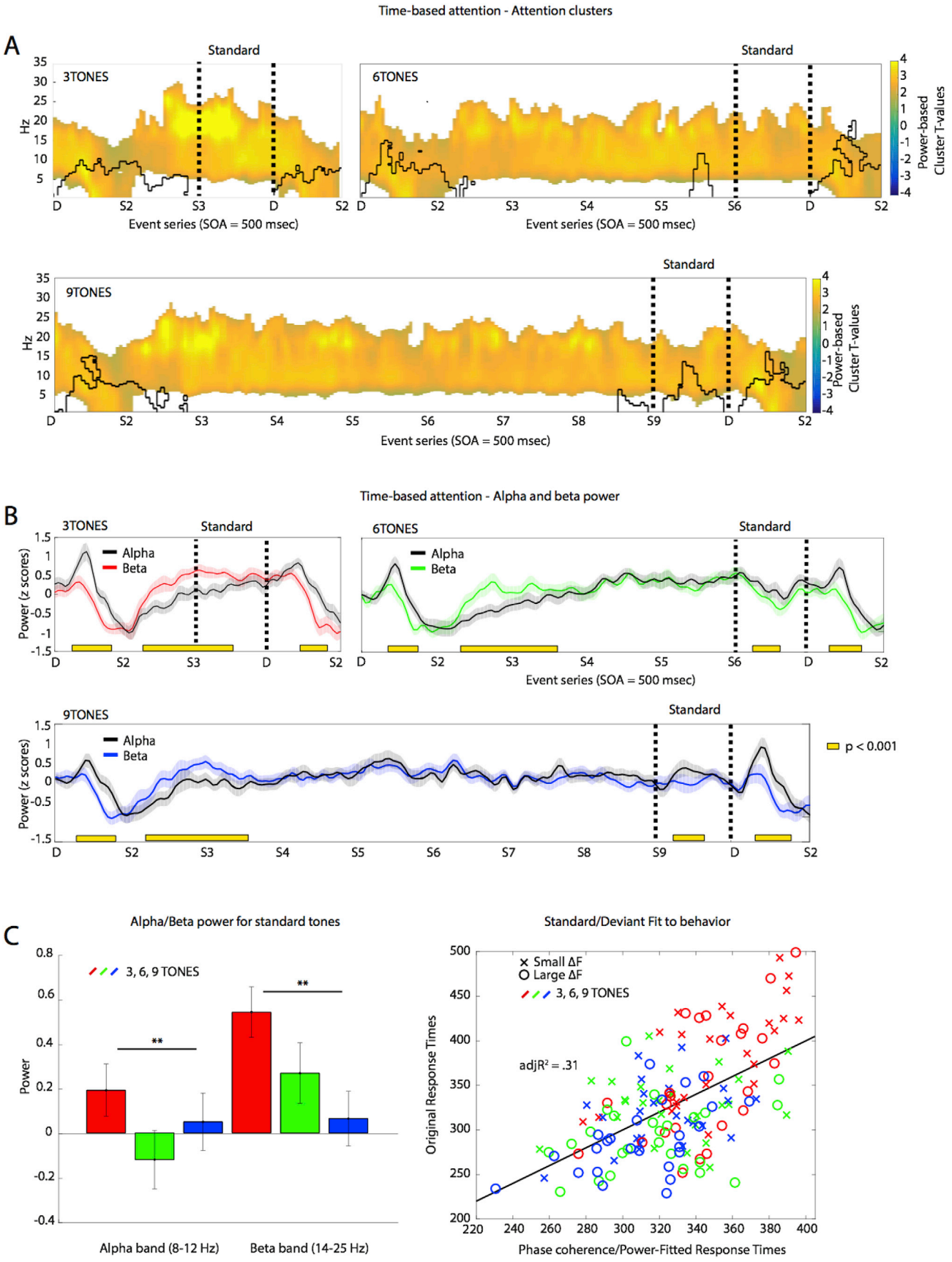

(caption on next page)

Fig. 4. Attention modulates elapsed time to the next deviant. A. Time-frequency clusters of significant differences in global power between Attentive and Pre-attentive conditions, for the three temporal expectation levels (upper layer for 3 and 6 tones, lower layer for nine tone), time-locked to the onset of the following deviant sound, plotted at the exemplar electrode Pz. The magnitude of statistical cluster differences is color-coded. Overlaid in black are the significant clusters for phase coherence. B. Average values across all electrodes of the standardized estimates of alpha (8–12 Hz) and beta (13–25 Hz) bands, derived from subtracting the activations in the Pre-attentive condition from those in the Attentive condition. Horizontal, yellow bars represent the extension in time of significant cluster differences between alpha and beta bands. C. Left panel, average power estimates for the last standard tone of each sequence, separately depicted the alpha and beta bands. Right panel, multiple regression model fit between attention-dependent phase coherence and power at deviant onset, attention-related alpha and beta power estimates for the last standard of each repetition series as predictor and response times as dependent viable. Fitted response times are plotted against original response times.

Importantly, this interval turned out to be behaviorally relevant, as a binomial test showed that it contained 100% of individual mean response time values (all $ps < 0.001$). The relative weight of alpha and beta signals flipped with a faster rebound of the beta band after the second tone in a series (S2). To quantify the dynamics of alpha and beta band while waiting for the deviant to occur, we calculated the median difference in power within the standard tone window (last tone of each series, 500-ms duration) between the Attentive and Pre-attentive conditions for both alpha and beta bands, across all electrodes, and entered them in a 2×3 rmANOVA with Band (Alpha vs. Beta) and Time (3TONES, 6TONES, and 9TONES) factors. There resulted a significant main effect of Time ($F(2,48) = 9.42$, $p < 0.001$, $\eta^2 = 0.28$), but no significant effect of Band or interaction (all $Fs \geq 4$, all $ps > 0.05$). Alpha and Beta band mean power for the 3TONES standards (mean = 0.39, SEM = 0.10) was significantly different from mean power for 6TONES standards (mean = 0.08, SEM = 0.13) and 9TONES standard (mean = 0.06, SEM = 0.12; see Fig. 4C, left panel). We then averaged across median alpha and beta power for standards, and entered the resulting estimates together with the difference in phase coherence and power between Attentive and Pre-attentive conditions at deviant onset obtained in the preceding section, as predictors of response times in a multiple regression. There resulted a significant model ($F_{(3,146)} = 24.01$, $p < 0.001$), explaining a more sizeable portion of the variance in the data (adjusted$R^2 = 0.31$). Notably, all predictors significantly contributed: Alpha/beta power for standard tones (standardized coefficient = 40.86, p = 0.025), phase coherence for deviant tones (standardized coefficient = - 399.77, $p < 0.001$), and global power for deviant tones (standardized coefficient = - 0.80, $p < 0.01$). Finally, we calculated log-likelihood function values for the multiple regression model with phase coherence for deviants as predictor (deviant-only model), as well as for the multiple regression model with phase coherence and power for deviants, plus averaged alpha and beta power for standards as predictors (deviant-and-standard model). The Akaike information criteria showed that the deviant-and-standard model resulted in a better fit (deviant-only fit, one parameter = 2060.8; deviant-and-standard model, three parameters = 2048.2).

4. Discussion

We tested how components of attention determine response behavior to pitch deviants in a sound stream. Deviants were unpredictable both in magnitude of change (Feature dimension) and as to the time at which they would appear (Time dimension). We found that the feature component ("what", reflecting deviancy magnitude) and the time component ("when", reflecting waiting time to the next deviant) separately predict response times. Moreover, for the deviant response, global power estimates were not discriminative of either the feature or time components, although attention generally enhanced power at deviant onset. Phase coherence, instead, predominantly encoded deviancy magnitude with a large effect size, although it also reflected the evolving temporal expectations (Time dimension), again as independent predictors of response times. Attention amplified phase coherence more strongly for large rather than small deviancy events, in line with the literature (Alho, 1992; Amenedo and Escera, 2000; Berti and Schröger, 2001; Tiitinen et al., 1994). Furthermore, the generation of temporal expectation effects on phase coherence was essentially due to the orienting of attention, rather than to the implicit learning of stimulus structure. Notably, attention-driven differences between large and small deviancy events were significantly encoded by phase coherence, confirming previous findings in pre-attentive experimental settings (Fuentemilla et al., 2008, 2006; Haenschel et al., 2000), as well as in attentive settings (Barne et al., 2017; Auksztulewicz and Friston, 2015). The largest differences were found for delta and theta bands (1–7 Hz; for an interaction of delta band modulation and temporal expectations in perception, see Herrmann et al., 2016). The brain-behavior model based on brain activity at deviant onset with global power and phase coherence predictors was significant but explained a moderate portion of the variance (21%), suggesting that it captured the general trend well, but the variance in response time poorly. Importantly, however, a cluster-based approach showed that the influence of attention on power estimates at deviant onset began already in the pre-stimulus interval, suggesting it is not specific to feature change. Indeed, we then analyzed the effects on attention on the waiting time series, we found a predominant power change at higher frequencies (alpha, 8–12 Hz, and beta, 13–25 Hz). Including power estimates for alpha/beta activity for the last tone of each waiting time series (Standard) made the model significantly more precise (31%). Notice that alpha/beta oscillatory power dynamics significantly contributed to modelling behavior.

Previous work on alpha and beta rhythms separately showed their importance for the deployment of attention in time. Our findings extend the relevance the alpha modulations for orienting of attention in time to continuous sequences of events. However, contrary to Rohenkohl and Nobre (2011), we found alpha to increase for short waiting times, and remain at plateau with a potential monitoring function for longer waiting times. At plateau, beta band power changes jointly with the alpha band, however it rebounds more rapidly than alpha power after deviant onset. We hypothesize that this difference could underlie a mechanistic explanation for why short waiting times are detrimental to response speed. If a decrease in cortical beta activity relates to the release of motor programs for button press (Joundi et al., 2013; Morillon and Baillet, 2017; Pfurtscheller et al., 2003; Pogosyan et al., 2009; Swann et al., 2009), then its relative faster rebound would make motor responses immediately following a deviant-dependent desynchronization simply harder to execute. Thus, we suggest that the point is *not* a facilitation of longer waiting times, as it is generally assumed – in fact, response times at 6-tone series and 9-tone series were similar –, but a disadvantage in responding at shorter intervals. This is also supported by the finding that all valid response times are subtended by the post-deviant time lag in which the alpha signal synchronizes while the beta signal desynchronizes (Wessel and Aron, 2017).

It generally remains an open question which particular aspects of behavior alpha and beta rhythms track, distinctly or jointly (Arnal and Giraud, 2012; Fujioka et al., 2015; Rohenkohl and Nobre, 2011; Sedley et al., 2016; Wilsch et al., 2014). Recent connectivity analysis work suggests that both alpha and beta are 'top-down' rhythms (Michalareas et al., 2016). According to Sedley et al. (2016), alpha and beta rhythms have concurrent functions: alpha relates to the precision of temporal predictions, while beta conveys changes in predictive strength. Spitzer and Haegens (2017) suggest that while alpha activity serves the function of suppressing irrelevant sensory processing, beta band modulations would foster the endogenous re-activation of task-specific information, by creating dedicated cell assemblies of short duration, extending the view on beta as a top-down rhythm, initially put forward by Engel and Fries (2010). Spitzer and Haegens' (2017) proposal also fits as an explanation for the dynamics of alpha and beta power that we described,

particularly for deviant onset – beta band activity is rapidly suppressed, since top-down predictions are violated, and alpha rhythm is enhanced, suppressing irrelevant sensory processing. We suggest that the onset of a new event inhibits the temporal dimension of attention to stimuli at higher frequencies, while boosting phase concentration at lower frequencies to better encode stimulus features, suggesting a division of neural labor for attention in complex sensory environments.

We also found that, for the longest waiting time in our sequences (4.5 s), temporal attention drove phase concentration in the standard period, as well as in the deviant period. In the longest waiting time condition, participants became confident about proximal target onset: the triggering of phase coherence mechanisms might serve to better encode the features of the standard stimulus in order to facilitate response speed. Fuentemilla et al. (2008) already found pre-attentive phase concentration for standard tones, but they used an oddball stimulus structure, collapsing standard tones at all durations. Furthermore, using a foreperiod experiment, Wilsch et al. (2015) found phase concentration in the lower delta band to increase with a longer waiting time to target, although their durations were similar to the 3TONE condition in our experiment, for which we found no phase concentration in the time dimension. This discrepancy could be accounted for by the fact that we investigated attentive modulation only (and at frequencies above 1 Hz), or by the sensory difference between classical foreperiod experiments, with silence between cue and target, and continuous stimulation as in our experiment.

We did not find any significant interaction between the behavioral components of Feature and Time, or their underlying neural processes. This is in line with the results of Auksztulewicz et al. (2018), who analyzed evoked responses in humans using invasive electrocorticography: their work suggests that predicting “what’ relies on short-term plasticity in sensory-specific areas, while predicting “when” depends on synaptic gain in motor areas. However, an interaction between feature-based and time-based dimensions of attention has been shown in animal studies (Jaramillo and Zador, 2011). In an experiment using temporally regular vs. irregular stimulation sequences, Cravo et al. (2013) showed that the phase of delta rhythm (1–4 Hz) in the temporally regular condition correlated with a gain in perceptual accuracy. By analogy, longer waiting times could have led to larger phase coherence in the delta and theta frequency bands for large deviancy events, or rather supported the processing of small deviancy events, by increasing the signal-to-noise ratio of their encoding (Okamoto et al., 2007). Contrary to this, we found that attention, and not waiting time, amplified phase coherence for large deviancy more than for small deviancy events. Attention had a similar effect on phase coherence for mounting temporal expectations. In a foreperiod GO-NO GO study, Cravo et al. (2011) positively linked power in the theta band with high temporal expectations. However, we found significant attention-related power differences only at higher frequencies. The absence of an interaction could be due to the differential weight of unpredictability in the Time and Feature dimensions: time-wise, unpredictability is only verified at the beginning of each standard series, as deviant onset becomes ever more probable with elapsed time, while unpredictability in the Feature dimension remains constant across each standard series.

A limitation to our study is that we could not rely on source localization techniques, due to the sparse electrode scalp coverage, and lack of structural information on individual brains. Further, we did not consider the dynamics of different components of the beta rhythm: low beta, or beta 1, between 14 and 19 Hz, vs. high beta, or beta 2, >20 Hz (see Kopell et al., 2011). Beta 2 is considered more specifically motor in origin and function (Brovelli et al., 2004), and thus its suppression might contribute more to the dynamic profile we highlighted. Finally, while we assume that participants are using elapsed time to compute the hazard rate, we cannot yet determine which level of the computation process is reflected by the neural indexes we analyzed, whether it is elapsed time *per se* or perceived event probability.

Our results suggest a division of neural labor between phase coherence at low frequencies and oscillatory power at high frequencies in encoding two components of sensory attention: capture by salient feature change, and the orienting in time to the next salient event.

Declarations of interest

None.

Acknowledgements

The authors received valuable help from the scientific staff at Max Planck Institute of Empirical Aesthetics, Frankfurt am Main (Germany): Dr. Cornelius Abel, MSc. Freya Materne, Dipl. Claudia Leher, Dr. Alexander Lindau, Dr. Wolf Schlotz. In particular, the authors are thankful to Dr. Cornelius Abel for helpful critical feedback. The project is supported by the Max Planck Society, Germany.

References

Alho, K., 1992. Selective attention in auditory processing as reflected by event-related brain potentials. Psychophysiology 29, 247–263.
Amenedo, E., Escera, C., 2000. The Accuracy of Sound Duration Representation in the Human Brain Determines the Accuracy of Behavioural Perception, vol. 12, pp. 2570–2574.
Arnal, L.H., Giraud, A., 2012. Cortical oscillations and sensory predictions. Trends Cognit. Sci. 1–9. https://doi.org/10.1016/j.tics.2012.05.003.
Auksztulewicz, R., Friston, K., 2015. Attentional enhancement of auditory mismatch responses: a DCM/MEG study. Cerebr. Cortex 25, 4273–4283.
Auksztulewicz, R., Schwiedrzik, C.M., Thesen, T., Doyle, W., Devinsky, O., Nobre, A.C., Schroeder, C.E., Friston, K.J., Melloni, L., 2018. Not all predictions are equal: "what" and "when" predictions modulate activity in auditory cortex through different mechanisms. J. Neurosci. 38, 8680–8693.
Baldeweg, T., Williams, J.D., Gruzelier, J.H., 1999. Differential changes in frontal and sub-temporal components of mismatch negativity. Int. J. Psychophysiol. 33, 143–148. https://doi.org/10.1016/S0167-8760(99)00026-4.
Barne, L.C., Maurice, P., Claessens, E., Reyes, M.B., Caetano, M.S., Cravo, A.M., 2017. NeuroImage Low-frequency cortical oscillations are modulated by temporal prediction and temporal error coding. Neuroimage 146, 40–46. https://doi.org/10.1016/j.neuroimage.2016.11.028.
Bell, A.J., Sejnowski, T.J., 1995. An information-maximization approach to blind separation and blind deconvolution. Neural Comput. 7, 1129–1159.
Bertelson, P., Boons, J.-P., 1960. Time uncertainty and choice reaction time. Nature 187, 531–532. https://doi.org/10.1038/187531a0.
Berti, S., Schröger, E., 2001. A comparison of auditory and visual distraction: behavioral and event-related indices. Cogn. Brain Res. 10, 265–273.
Brainard, D.H., 1997. The psychophysics toolbox. Spatial Vis. 10, 433–436.
Brovelli, A., Ding, M., Ledberg, A., Chen, Y., Nakamura, R., Bressler, S.L., 2004. Beta oscillations in a large-scale sensorimotor cortical network: directional influences revealed by Granger causality. Proc. Natl. Acad. Sci. USA. 101, 9849–9854.
Chaumon, M., Bishop, D.V., Busch, N.A., 2015. A practical guide to the selection of independent components of the electroencephalogram for artifact correction. J. Neurosci. Methods 250, 47–63.
Correa, Á., Lupiáñez, J., Milliken, P., Tudela, P., 2004. Endogenous temporal orienting of attention in detection and discrimination tasks. Percept. Psychophys. 66, 264–278.
Costa-faidella, J., Baldeweg, T., Grimm, S., Escera, C., 2011. Interactions between “ what ” and “ when ” in the Auditory System : Temporal Predictability Enhances Repetition Suppression, vol. 31, pp. 18590–18597. https://doi.org/10.1523/JNEUROSCI.2599-11.2011.
Cravo, A.M., Rohenkohl, G., Wyart, V., Nobre, A.C., 2011. Endogenous Modulation of Low Frequency Oscillations by Temporal Expectations, pp. 2964–2972. https://doi.org/10.1152/jn.00157.2011.
Cravo, A.M., Rohenkohl, G., Wyart, V., Nobre, A.C., 2013. Temporal expectation enhances contrast sensitivity by phase entrainment of low-frequency oscillations in visual cortex, 33, pp. 4002–4010. https://doi.org/10.1523/JNEUROSCI.4675-12.2013.Temporal.
Cui, X., Stetson, C., Montague, P.R., Eagleman, D.M., 2009. Ready ... Go: amplitude of the fMRI signal encodes expectation of cue arrival time. PLoS Biol. 7, e1000167.
Delorme, A., Makeig, S., 2004. EEGLAB: an open source toolbox for analysis of single-trial EEG dynamics. J. Neurosci. Methods 134, 9–21.
de Lange, F.P., Rahnev, D.A., Donner, T.H., Lau, H., 2013. Anticipation increases tactile stimulus processing in the ipsilateral primary somatosensory cortex. J. Neurosci. 33, 1400–1410.
Engel, A.K., Fries, P., 2010. Beta-band oscillations - signalling the status quo? Curr. Op. Neurobiol. 20, 156–165.
Fuentemilla, L., Marco-Pallarés, J., Grau, C., 2006. Modulation of spectral power and of phase resetting of EEG contributes differentially to the generation of auditory event-related potentials. Neuroimage 30, 909–916. https://doi.org/10.1016/J.NEUROIMAGE.2005.10.036.

Fuentemilla, L., Marco-Pallarés, J., Münte, T.F., Grau, C., 2008. Theta EEG oscillatory activity and auditory change detection. Brain Res. 1220, 93–101. https://doi.org/10.1016/J.BRAINRES.2007.07.079.

Fujioka, T., Ross, X.B., Trainor, L.J., 2015. Beta-Band Oscillations Represent Auditory Beat and its Metrical Hierarchy in Perception and Imagery, vol. 35, pp. 15187–15198. https://doi.org/10.1523/JNEUROSCI.2397-15.2015.

Grings, W.W., Dawson, M.E., 1978. Emotions and Bodily Responses: a Psychophysiological Approach. Academic Press, New York, USA.

Haenschel, C., Baldeweg, T., Croft, R.J., Whittington, M., Gruzelier, J., 2000. Gamma and beta frequency oscillations in response to novel auditory stimuli: a comparison of human electroencephalogram (EEG) data with in vitro models. Proc. Natl. Acad. Sci. U. S. A 97, 7645–7650. https://doi.org/10.1073/pnas.120162397.

Haenschel, C., Vernon, D.J., Dwivedi, P., Gruzelier, J.H., Baldeweg, T., 2005. Event-related brain potential correlates of human auditory sensory memory-trace. Formations 25, 10494–10501. https://doi.org/10.1523/JNEUROSCI.1227-05.2005.

Herrmann, B., Henry, M.J., Haegens, S., Obleser, J., 2016. Temporal expectations and neural amplitude fluctuations in auditory cortex interactively in fluence perception. Neuroimage 124, 487–497. https://doi.org/10.1016/j.neuroimage.2015.09.019.

Jaramillo, S., Zador, A.M., 2011. Auditory cortex mediates the perceptual effects of acoustic temporal expectation Santiago. Nat. Neurosci. 14, 246–251. https://doi.org/10.1038/nn.2688.

JASP Team, 2016. JASP (Version 0.8.0.1) ([Computer software]).

Joundi, R.A., Brittain, J.S., Green, A.L., Aziz, T.Z., Brown, P., Jenkinson, N., 2013. Persistent suppression of subthalamic beta-band activity during rhythmic finger tapping in Parkinson's disease. Clin. Neurophysiol. 124, 565–573.

Jung, T.-P., Humphries, C., Lee, T.W., Makeig, S., McKeown, M.J., Iragui, V., Sejnowski, T.J., 1998. Extended ICA removes artifacts from electroencephalographic recordings. Adv. Neural Inf. Process. Syst. 10, 894–900.

Kim, Y.J., Grabowecky, M., Paller, K.A., Muthu, K., Suzuki, S., 2007. Attention induces synchronization-based response gain in steady-state visual evoked potentials. Nat. Neurosci. 10, 117–125. https://doi.org/10.1038/nn1821.

Kopell, N., Whittington, M.A., Kramer, M.A., 2011. Neuronal assembly dynamics in the beta1 frequency range permits short-term memory. Proc. Natl. Acad. Sci. U. S. A. 108, 3779–3784.

Lakatos, P., Karmos, G., Mehta, A.D., Ulbert, I., Schroeder, C.E., 2008. Entrainment of neuronal oscillations as a mechanism of attentional selection. Science 320, 110–113.

Luce, R.D., 1986. Response times: their role in inferring elementary mental organization. Oxford University Press, Oxford.

Makeig, S., Westerfield, M., Jung, T.P., Enghoff, S., Townsend, J., Courchesne, E., Sejnowski, T.J., 2002. Dynamic brain sources of visual evoked responses. Science 295, 690–694.

Maris, E., Oostenveld, R., 2007. Nonparametric statistical testing of EEG- and MEG-data. J. Neurosci. Methods 164, 177–190.

Meck, W.H., 1988. Internal clock and reward pathways share physiologically similar information-processing pathways. In: Commons, M.L., Church, R.M., Stellar, J.R., Wagner, A.R. (Eds.), Quantitative Analyses of Behavior: Biological Determinants of Reinforcement. Lawrence Erlbaum, Hillsdale, NJ, pp. 121–138.

Michalareas, G., Vezoli, J., van Pelt, S., Schoffelen, J.M., Kennedy, H., Fries, P., 2016. Alpha-Beta and Gamma rhythms subserve feedback and feedforward influences among human visual cortical areas. Neuron 89, 384–397.

Morillon, B., Baillet, S., 2017. Motor origin of temporal predictions in auditory attention. Proc. Natl. Acad. Sci. U. S. A 114, E8913–E8921. https://doi.org/10.1073/pnas.1705373114.

Murray, M.M., Brunet, D., Michel, C.M., 2008. Topographic ERP analyses: a step-by-step tutorial review. Brain Topogrfuentemilla 20, 249–264.

Näätänen, R., 1992. Attention and Brain Function. Lawrence Erlbaum, Hillsdale, NJ.

Näätänen, R., Paavilainen, P., Rinne, T., Alho, K., 2007. The mismatch negativity (MMN) in basic research of central auditory processing: a review. Clin. Neurophysiol. 118, 2544–2590.

Niemi, P., Näätänen, R., 1981. Foreperiod and simple reaction time. Psychol. Bull. 89, 133–162.

Nobre, A., Correa, A., Coull, J., 2007. The hazards of time. Curr. Opin. Neurobiol. 17, 465–470.

Okamoto, H., Stracke, H., Wolters, C.H., Schmael, F., Pantev, C., 2007. Attention improves population-level frequency tuning in human auditory cortex. J. Neurosci. 27, 10383–10390.

Oostenveld, R., Fries, P., Maris, E., Schoffelen, J.M., 2011. FieldTrip: open source software for advanced analysis of MEG, EEG, and invasive electrophysiological data. Comput. Intell. Neurosci. 2011 https://doi.org/10.1155/2011/156869. Article ID 156869.

Pelli, D.G., 1997. The VideoToolbox software for visual psychophysics: transforming numbers into movies. Spatial Vis. 10, 437–442.

Pfurtscheller, G., Graimann, B., Huggins, J.E., Levine, S.P., Schuh, L.A., 2003. Spatiotemporal patterns of beta desynchronization and gamma synchronization in corticographic data during self-paced movement. Clin. Neurophysiol. 114, 1226–1236.

Pogosyan, A., Gaynor, L.D., Eusebio, A., Brown, P., 2009. Boosting cortical activity at Beta-band frequencies slows movement in humans. Curr. Biol. 19, 1637–1641.

Rahne, T., von Specht, H., Mühler, R., 2008. Sorted averaging. Application to auditory event-related responses. J. Neurosci. Methods 172, 74–78.

Ratcliff, R., 1993. Methods for dealing with reaction time outliers. Psychol. Bull. 114, 510–532.

Rohenkohl, G., Nobre, A.C., 2011. Alpha Oscillations Related to Anticipatory Attention Follow Temporal Expectations, vol. 31, pp. 14076–14084. https://doi.org/10.1523/JNEUROSCI.3387-11.2011.

Ruhnau, P., Herrmann, B., Schröger, E., 2012. Finding the right control: the mismatch negativity under investigation. Clin. Neurophysiol. 123, 507–512.

Sedley, W., Gander, P.E., Kumar, S., Kovach, C.K., Oya, H., Kawasaki, H., Iii, M.A.H., 2016. Neural Signatures of Perceptual Inference. E-Life, pp. 1–13. https://doi.org/10.7554/eLife.11476.

Southwell, R., Baumann, A., Gal, C., Barascud, N., Friston, K., Chait, M., 2016. Is predictability salient? A study of attentional capture by auditory patterns. Phil. Trans. R. Soc. B 372, 20160105.

Spitzer, B., Haegens, S., 2017. Beyond the status quo: a role for beta oscillations in endogenous content (Re)activation. In: eNeuro 4 pii: ENEURO.0170-17, 2017.

Stefanics, G., Hangya, B., Hernadi, I., Winkler, I., Lakatos, P., Ulbert, I., 2010. Phase entrainment of human delta oscillations can mediate the effects of expectation on reaction speed. J. Neurosci. 30, 13578–13585.

Sussman, E., Winkler, I., Huotilainen, M., Ritter, W., Näätänen, R., 2002. Top-down effects can modify the initially stimulus-driven auditory organization. Cogn. Brain Res. 13, 393–405.

Sussman, E.S., 2007. A new view on the MMN and attention debate: the role of context in processing auditory events. J. Psychophysiol. 21, 164–175.

Sussman, E.S., Chen, S., Sussman-Fort, J., Dinces, E., 2014. The five myths of MMN: redefining how to use MMN in basic and clinical research. Brain Topogr. 27, 553–564.

Swann, N., Tandon, N., Canolty, R., Ellmore, T.M., McEvoy, L.K., Dreyer, S., DiSano, M., Aron, A.R., 2009. Intracranial EEG reveals a time- and frequency-specific role for the right inferior frontal gyrus and primary motor cortex in stopping initiated responses. J. Neurosci. 29, 12675–12685.

Tallon-Baudry, C., Bertrand, O., Delpuech, C., Pernier, J., 1996. Stimulus specificity of phase-locked and non-phase-locked 40 Hz visual responses in human. J. Neurosci. 16, 4240–4249.

Tiitinen, H., May, P., Reinikainen, K., Näätänen, R., 1994. Attentive novelty detection in humans is governed by pre-attentive sensory memory. Nature. https://doi.org/10.1038/372090a0.

Urbach, T.P., Kutas, M., 2006. Interpreting event-related brain potential (ERP) distributions: implications of baseline potentials and variability with application to amplitude normalization by vector scaling. Biol. Psychol. 72, 333–343.

Vangkilde, S., Coull, J.T., Bundesen, C., 2012. Great expectations: temporal expectation modulates perceptual processing speed. J. Exp. Psychol. Hum. Percept. Perform. 38, 1183–1119.

Wagenmakers, E.J., 2007. A practical solution to the pervasive problems of p values. Psychon. Bull. Rev. 14, 779–804.

Widmann, A., Schröger, E., Maess, B., 2015. Digital filter design for electrophysiological data – a practical approach. J. Neurosci. Methods 250, 34–46.

Wessel, J.R., Aron, A.R., 2017. On the globality of motor suppression: unexpected events and their influence on behavior and cognition. Neuron 93, 259–280. https://doi.org/10.1016/j.neuron.2016.12.013.

Wilsch, A., Henry, M.J., Herrmann, B., Maess, B., Obleser, J., 2014. Slow-delta phase concentration marks improved temporal expectations based on the passage of time. Psychophysiology 52, 910–918.

Wilsch, A., Henry, M.J., Herrmann, B., Maess, B., Obleser, J., 2015. Alpha oscillatory dynamics index temporal expectation benefits in working memory. Cerebr. Cortex 25, 1938–1946.

Woodrow, H., 1914. The measurement of attention. Psychol. Monogr. 17, 5.